Edinburgh 2012/14

arXiv:1207.0445v1 [hep-ph] 2 Jul 2012

General dissipation coefficient in low-temperature warm inflation

Mar Bastero-Gil,[1,*] Arjun Berera,[2,†] Rudnei O. Ramos,[3,‡] and João G. Rosa[2,§]
[1]*Departamento de Física Teórica y del Cosmos, Universidad de Granada, Granada-18071, Spain*
[2]*SUPA, School of Physics and Astronomy, University of Edinburgh, Edinburgh, EH9 3JZ, United Kingdom*
[3]*Departamento de Física Teórica, Universidade do Estado do Rio de Janeiro, 20550-013 Rio de Janeiro, RJ, Brazil*

(Dated: July 3, 2012)

In generic particle physics models, the inflaton field is coupled to other bosonic and fermionic fields that acquire large masses during inflation and may decay into light degrees of freedom. This leads to dissipative effects that modify the inflationary dynamics and generate a nearly-thermal radiation bath, such that inflation occurs in a warm rather than supercooled environment. In this work, we perform a numerical computation and obtain expressions for the associated dissipation coefficient, focusing on the regime where the radiation temperature is below the heavy mass threshold, while allowing for generic couplings and field multiplicities. We also discuss radiative corrections to particle masses and decay widths and how they may significantly increase the effects of dissipation.

I. INTRODUCTION

Inflation [1] is an extremely successful paradigm providing an elegant solution to the shortcomings of the standard cosmological model, in particular explaining the high degree of flatness and homogeneity of the observable universe, as well as describing the origin of the temperature anisotropies observed in the Cosmic Microwave Background and the seeds of the Large Scale Structure of our universe.

In the traditional picture of inflation, the early universe is dominated by the vacuum energy of a scalar field ϕ that slowly rolls down its potential, $V(\phi)$. This mimics the effect of a cosmological constant if the kinetic energy of the inflaton field is negligible, a condition that is necessarily violated at some point during the evolution of the field towards the minimum of the potential, thus yielding a finite period of accelerated expansion. This typically requires a scalar field with extremely weak self-interactions, so that its very flat potential leads to 40-60 e-folds of inflation.

The quasi-exponential expansion redshifts away any matter or radiation present before the scalar field comes to dominate the energy density:

$$\dot{\rho}_R + 4H\rho_R = 0 \qquad \Rightarrow \qquad \rho_R \sim e^{-4Ht} \ , \tag{1.1}$$

and consequently one needs a mechanism to reheat the cold inflationary universe and provide an exit into the standard radiation-dominated cosmology. The inflaton field must thus have some interactions with other fields, which directly or indirectly lead to the production of at least the Standard Model degrees of freedom and the particles that presumably constitute the inferred dark matter content of our universe.

These interactions must, however, be sufficiently weak in order to preserve the flatness of the inflaton potential at the quantum level, which can be achieved by either (fine-)tuning the associated couplings or by considering additional symmetries that, in particular, keep the mass of the scalar inflaton below the value of the Hubble parameter during inflation, thus ensuring an overdamped evolution. Moreover, when one considers generic couplings to additional scalar (fermionic) fields of the form $g^2\phi^2\chi^2$ ($g\phi\bar{\psi}\psi$), these fields typically become heavy during inflation due to the large values of the inflaton vacuum expectation value (vev). This implies that the decays $\phi \to \chi\chi, \bar{\psi}\psi$ are generically forbidden in the slow-roll regime, with reheating of these degrees of freedom occuring naturally only at the end of inflation if the inflaton vev drops sufficiently.

Interactions with additional scalar fields may also have interesting dynamical consequences, as is the case of hybrid inflation models [2, 3], where negative contributions to the squared mass of the waterfall field χ, coupled to the inflaton as above, make it tachyonic at some critical value of ϕ. Inflation then ends with a phase transition in which the χ-field evolves towards the true minimum of its potential, and in the process it may reheat the universe if it is coupled to radiation.

---

[*] Electronic address: mbg@ugr.es
[†] Electronic address: ab@ph.ed.ac.uk
[‡] Electronic address: rudnei@uerj.br
[§] Electronic address: joao.rosa@ed.ac.uk

Warm inflation [4, 5] (see also [6]) provides an alternative picture of the inflationary universe, in which particle production is sourced by the rolling inflaton field itself, so that radiation is not completely diluted away:

$$\dot{\rho}_R + 4H\rho_R = \Upsilon\dot{\phi}^2 \qquad \Rightarrow \qquad \rho_R \to \frac{\Upsilon\dot{\phi}^2}{4H} \sim const. \,, \tag{1.2}$$

in the slow-roll regime. Although accelerated expansion only occurs for a sub-dominant radiation component, $\rho_R \ll \rho_\phi$, it is possible that its temperature exceeds the de Sitter temperature, $T > H$, which significantly changes the inflationary dynamics[1]. On one hand, the spectrum of primordial density fluctuations is seeded by thermal rather than vacuum fluctuations of the inflaton field [4, 7–10], which my lead to interesting observational consequences such as the suppression of the tensor-to-scalar ratio and significant deviations from a gaussian spectrum [11–14]. On the other hand, particle production induces an additional friction term in the inflaton's motion:

$$\dot{\rho}_\phi + 3H(\rho_\phi + p_\phi) = -\Upsilon\dot{\phi}^2 \,, \tag{1.3}$$

which using $\rho_\phi = \dot{\phi}^2/2 + V(\phi)$ and $p_\phi = \dot{\phi}^2/2 - V(\phi)$ leads to:

$$\ddot{\phi} + 3H\dot{\phi} + V_\phi = -\Upsilon\dot{\phi} \,, \tag{1.4}$$

where V_ϕ denotes the derivative of the inflaton potential. This friction then contributes to overdamp the inflaton's motion, alleviating the need for very finely-tuned flat potentials (see e.g. [15]). This may be particularly relevant for supergravity and string theory models [16, 17], where one typically finds $m_\phi \gtrsim H$, precluding a sufficiently long period of inflation.

We are mainly interested in dissipative effects in the *adiabatic* regime, where the microscopic particle dynamics is much faster than the evolution of any macroscopic variable, which typically holds during slow-roll inflation. The calculation of dissipation coefficients in the adiabatic regime has been a long studied problem in quantum field theory, starting primarily with the seminal works in the 80's of Hosoya and Sakagami [18] for the ϕ^4 interaction (see also [19]). This was followed by Morikawa [20], who used the Closed Time Path formalism and obtained an effective Langevin-like equation, including an explicit fluctuation-dissipation relation. Fluctuation-dissipation relations emerging from quantum field theory models have since been examined by several other authors [21–24]. Initially these treatments considered weak dissipation, leading to an underdamped evolution, although it was subsequently shown in [25] that strong dissipation with overdamped trajectories could also be achieved. All these studies were performed in Minkowski spacetime and one of the first to consider dissipation in curved spacetime was Ringwald [26], with other subsequent treatments such as [27–29]. Dissipation from quantum field theory models has in fact been considered for a variety of applications beyond warm inflation dynamics, such as phase transitions, heavy ion collisions and conventional reheating after inflation.

For the reasons described above, the interactions between the inflaton and the radiation must be sufficiently suppressed to maintain the flatness of the potential, and in particular the finite temperature of the radiation may induce large thermal corrections to the inflaton mass, with $m_\phi \sim T > H$. This in fact precludes successful realizations of warm inflation in the simplest models, with the inflaton coupled directly to light scalars or fermions as described above, as the additional friction cannot overcome the increase in the inflaton's mass [25, 30]. This of course assumes these are relativistic degrees of freedom, with $T \gg m_{\chi,\psi}$, but, as previously discussed, fields which are directly coupled to the inflaton tend to acquire large masses during inflation.

This has motivated implementations of warm inflation scenarios in the low-temperature regime, with $m_{\chi,\psi} < T$ (see e.g. [31] for other recent implementations of warm inflation). In this case the on-shell production of these degrees of freedom is Boltzmann-suppressed, but contributions from virtual modes may still lead to significant dissipative effects if the fields have a finite decay width. In fact, this scenario, proposed in [32] and suggestively known as the *two-stage mechanism*, has all the ingredients of hybrid inflation models, where it is the waterfall field and not the inflaton that interacts with and may decay into light degrees of freedom. Moreover, it has been shown that the inclusion of both bosonic and fermionic degrees of freedom in a supersymmetric theory may help controlling both radiative and thermal corrections to the inflaton potential, despite supersymmetry being broken by both the finite energy density and the finite temperature during warm inflation [33].

In this work, we extend earlier computations of the dissipation coefficient Υ in the low-temperature regime [34, 35] for the case where the fields coupled to the inflaton have a large decay width, where one expects particle production to be more efficient. Although most computations have to be performed numerically in this regime, our goal is to provide accurate expressions for Υ that may be used in constructing models of warm inflation for a broad range of field masses and couplings.

---

[1] In this work we will consider a radiation bath that is close to thermal equilibrium, although this need not be the case in general.

Our work is organized as follows. In the next section we describe the interactions between the inflaton field, the heavy fields and the light degrees of freedom that make up the radiation bath. We then discuss the leading thermal corrections to the particle masses for weak and strong couplings, which may be found in Section III. In Section IV, we describe the computation of the dissipation coefficient in the low-temperature regime and determine its dependence on the particle masses and couplings by fitting our numerical results to well-motivated expressions. Finally, in Section V we estimate the effects of higher-order radiative corrections to the decay width of the heavy fields and discuss their implications for warm inflation model building. We summarize our main results and conclusions in Section VI.

II. SUPERSYMMETRIC MODEL

We consider a generic supersymmetric model with chiral superfields Φ, X and Y_i, $i = 1, \ldots, N_Y$, described by the superpotential [15, 33]:

$$W = \frac{g}{2}\Phi X^2 + \frac{h_i}{2} X Y_i^2 + f(\Phi) \ , \tag{2.1}$$

where a sum over the index i is implicit. The scalar component of the superfield Φ describes the inflaton field, with an expectation value $\phi = \varphi/\sqrt{2}$, which we assume to be real, and the generic holomorphic function $f(\Phi)$ describes the self-interactions in the inflaton sector. The structure of the superpotential is quite generic in renormalizable models, following from the simple assumption that not all degrees of freedom are directly coupled to the inflaton field, and may for example be naturally implemented in D-brane constructions and related gauge theories (see e.g. [17] and references therein). The analysis that we will go through below concentrates mostly on the scalar and fermionic sectors, which are already sufficiently involved, but we discuss the possibility of embedding this superpotential in a gauge theory in Section VI.

The Lagrangian density describing the interactions between the inflaton vev and the scalar components of the superfields X and Y_i, denoted by χ and σ_i, respectively, is given by:

$$\begin{aligned}\mathcal{L}_{scalar} &= V(\varphi) + \frac{1}{2}g^2\varphi^2|\chi|^2 + \frac{g}{2}\sqrt{V(\varphi)}\left(\chi^2 + \chi^{\dagger 2}\right) + \frac{g^2}{4}|\chi|^4 + \\ &+ \frac{h_i}{2}\frac{g\varphi}{\sqrt{2}}\left(\chi\sigma_i^{\dagger 2} + \chi^\dagger \sigma_i^2\right) + \frac{h_i h_j}{4}\sigma_i^2\sigma_j^{\dagger 2} + h_i^2|\chi|^2|\sigma_i|^2 \ ,\end{aligned} \tag{2.2}$$

where $V(\varphi) = |f'(\phi)|^2$ is the potential driving inflation. Similarly, the interactions involving the fermionic components ψ_χ and ψ_{σ_i} and the scalar inflaton are given by:

$$\mathcal{L}_{fermion} = \frac{1}{2}\frac{g\varphi}{\sqrt{2}}\bar{\psi}_\chi P_L \psi_\chi + \frac{h_i}{2}\chi\bar{\psi}_{\sigma_i} P_L \psi_{\sigma_i} + h_i\sigma_i\bar{\psi}_{\sigma_i} P_L \psi_\chi + \text{h.c.} \ , \tag{2.3}$$

where $P_L = (1-\gamma_5)/2$ is the left-handed chiral projector. Note that for our study of the dissipative dynamics during inflation we are only interested in the interactions involving the inflaton vev, but one should take into account that there are also interactions involving scalar fluctuations about the background value and their fermionic superpartners, although, for simplicity, we do not write them explicitly in Eqs. (2.2) and (2.3). Also, for the purposes of this work, we will assume that the couplings g and h_i are real, although complex couplings may play an important role in, for example, generating a baryon asymmetry through dissipative effects during warm inflation [36].

From the interactions shown in Eqs. (2.2) and (2.3), we can see that the fields in the X multiplet, which are directly coupled to the inflaton in the superpotential, acquire tree-level masses that are generically large for large values of the inflaton vev. On the other hand, the fields in the Y_i multiplets remain massless at tree-level, although we may in general consider an additional mass term for these fields, which we will assume to be small compared to the temperature scale during inflation, an issue we will return to in the next section. The non-vanishing potential energy driving inflation breaks supersymmetry, which leads to a mass splitting in the scalar sector of the X multiplet:

$$\begin{aligned} m_{\chi_{R,I}}^2 &= \frac{g^2\varphi^2}{2}\left(1 \pm \frac{\sqrt{V(\varphi)}}{g\varphi^2}\right) \ , \\ m_{\psi_\chi}^2 &= \frac{g^2\varphi^2}{2} \ , \end{aligned} \tag{2.4}$$

where $\chi = (\chi_R + i\chi_I)/\sqrt{2}$. Due to the smallness of the inflaton self-interactions typically required for a sufficiently long period of slow-roll inflation and a small enough amplitude for the spectrum of primordial density perturbations, this splitting may in general be neglected during inflation. For example, for $V(\varphi) = \lambda^2\varphi^4$, the splitting factor is $1 \pm \lambda/g$, with the primordial spectrum imposing $\lambda \sim 10^{-7}$, so that we generically expect $\lambda \ll g$ (see e.g. [15]). Henceforth we will then consider a common mass $m_\chi = g\varphi/\sqrt{2}$ for all fields in the X multiplet. If the inflaton vev is sufficiently large, this mass will be above the temperature of the radiation bath during warm inflation, in which case thermal contributions to the inflaton mass from χ and ψ_χ loops are Boltzmann-suppressed, $e^{-m_\chi/T} \ll 1$, and do not destroy the flatness of the tree-level potential.

This mass splitting may nevertheless be important when computing radiative corrections to the inflaton potential, and the supersymmetric Coleman-Weinberg potential has been shown to yield [33]:

$$V_{CW} = \frac{1}{32\pi^2}\mathrm{Str}\left[\mathcal{M}_X^4\left(\log\left(\frac{\mathcal{M}_X^2}{\mu^2}\right) - \frac{3}{2}\right)\right] \simeq \frac{g^2}{32\pi^2}V(\varphi)\log\left(\frac{m_\chi^2}{\mu^2}\right) , \tag{2.5}$$

where μ is the renormalization scale and we have taken the leading correction from supersymmetry breaking. This shows that the leading radiative corrections to the inflaton potential are logarithmic and hence will not spoil the flatness of the potential for $g \lesssim 1$. Note that if we consider N_X multiplets coupled to the inflaton as in Eq. (2.1), the radiative corrections will be proportional to $g^2 N_X$, and this may still accommodate a moderately large field multiplicity without a significant tuning of the coupling constant.

One should also notice that in some cases the mass splitting induced by supersymmetry breaking may actually become relevant at the end of the inflationary evolution. For example, for $f(\Phi) = gM^2\Phi$, we have $V(\varphi) \simeq g^2M^4$ and $m_{\chi_{R,I}}^2 = m_\chi^2 \pm M^2/2$, so that the imaginary component becomes tachyonic for $\varphi < M$, leading to a phase transition that ends inflation in the conventional hybrid mechanism.

The superpotential (2.1) is thus a simple generalization of supersymmetric hybrid inflation that allows for an arbitrary inflaton potential and additional couplings of the waterfall field(s) to other scalars and fermions. These couplings allow for the decays $\chi \to \sigma\sigma, \psi_\sigma\psi_\sigma$ and $\psi_\chi \to \sigma\psi_\sigma$, as can be easily seen from Eqs. (2.2) and (2.3), and thus allow the waterfall field and its superpartners to 'reheat' the universe after the hybrid transition. Most importantly, even though the fields in the X-multiplet are too heavy to be produced on-shell during inflation, virtual χ and ψ_χ pairs can be produced from the rolling inflaton field and may in turn decay into the Y_i-multiplet particles, leading to dissipative particle production and to the two-stage realization of warm inflation [32], which will be main topic of this work.

The scalar and fermionic Lagrangian densities also include interactions involving the fields in the X and Y_i multiplets that play an important role in the dynamics of warm inflation, not only by contributing to the thermal masses of these fields, as we will analyze in the next section, but also by allowing thermal scatterings that keep the system close to thermal equilibrium. For example, the cross-section for thermal scatterings of the complex light scalars σ_i includes contributions from $\sigma_i\sigma_i \to \sigma_j\sigma_j$ and $\sigma_i\sigma_i^\dagger \to \sigma_i\sigma_i^\dagger$, being given by:

$$\sigma_{th}^i = \frac{h^4(N_Y + 2)}{32\pi s} , \tag{2.6}$$

where $\sqrt{s}$ is the centre-of-mass energy and we have assumed $h_i = h$ for all species, which for simplicity we will consider in the remainder of our discussion. For $\sqrt{s} \sim T$ during warm inflation, this yields a scattering rate:

$$\frac{\Gamma_{th}^i}{H} = \frac{\langle\sigma_{th}^i n_i v\rangle}{H} \sim \frac{\zeta(3)}{8\pi^3}h^4(N_Y + 2)\left(\frac{T}{H}\right) \simeq 121\left(\frac{h}{4\pi}\right)^4 N_Y\left(\frac{T}{H}\right) , \tag{2.7}$$

for $N_Y \gg 1$, so that we expect $\Gamma_{th}^i \gtrsim H$ for $T \gtrsim H$ and perturbative couplings. On the other hand, fermionic species can only interact with each other or their scalar superpartners via the exchange of virtual χ, ψ_χ-modes, with scattering rates thus suppressed by a factor $(T/m_\chi)^4 \ll 1$. As we shall discuss below, fermionic contributions to the dissipation coefficient are also suppressed by similar factors, so that we expect fermions to be a negligible component of the radiation bath, a symptom of supersymmetry breaking during warm inflation.

III. THERMAL MASS CORRECTIONS

The two-stage interactions between the inflaton and X and Y_i fields leads to the formation of a thermal bath during inflation, and finite temperature effects may thus become important. Since χ and ψ_χ acquire large tree-level masses and we assume $T \ll m_\chi$, their contributions to thermal loop corrections are Boltzmann-suppressed and may be ignored. This precludes large thermal mass corrections not only to the inflaton field but also to the light σ and ψ_σ particles that form the radiation bath.

The masses of both the bosonic and fermionic components of the X-multiplet receive nevertheless corrections from their interactions with the light fields, the leading diagrams being illustrated in Fig. 1.

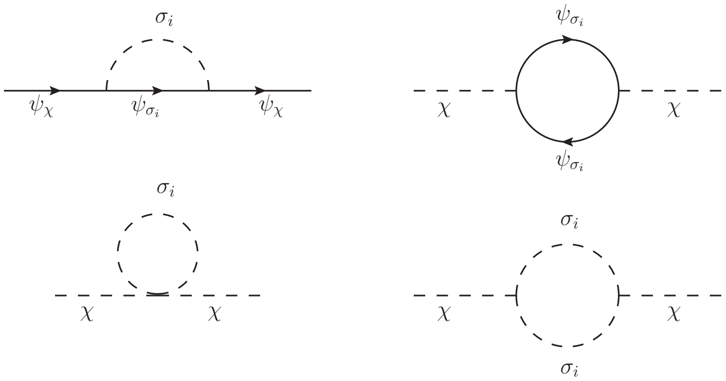

FIG. 1: Feynman diagrams contributing to the self-energy of the ψ_χ and χ fields to leading order. Note that the last diagram corresponds to an effective finite temperature contribution to the coupling $g(T)$ rather than a thermal mass correction [33].

These have been computed in [33] and are identical for both bosonic and fermionic degrees of freedom. Taking into account our normalization of the couplings in the superpotential (which differs from [33], by a factor 1/2) and the field multiplicity, this yields the renormalized mass:

$$\tilde{m}_\chi^2 = m_\chi^2 + \frac{h^2 N_Y}{8} T^2 \ . \tag{3.1}$$

In particular, this implies that the one-loop effective potential at finite temperature can be obtained by replacing the tree-level mass by $\tilde{m_\chi}$ in Eq. (2.5). This shows that the leading thermal corrections to the inflaton potential are logarithmic and that, for $T \ll m_\chi$, they are smaller than the zero-temperature radiative corrections induced by the inflaton vev. We will nevertheless include these corrections in the computation of the dissipation coefficient.

In the Y_i-sector, the light σ_i scalars receive thermal corrections from their self-interactions, while their superpartners only have couplings involving at least one heavy field, and thermal loop contributions are thus suppressed in this case. The leading diagrams contributing to the scalar masses are shown in Fig. 2.

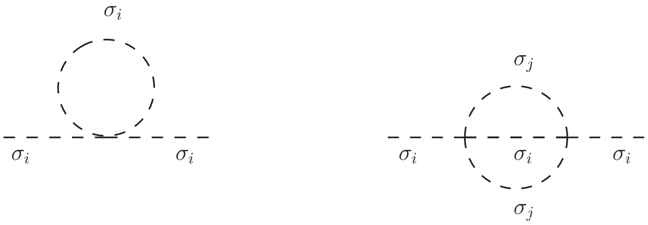

FIG. 2: Feynman diagrams contributing to the self-energy of the σ_i fields to leading order. Note that the 'sunset' diagram on the right gives the leading-order correction involving different light species.

The leading corrections to the mass of each species σ_i correspond to the quartic self-interactions $(h_i^2/4)|\sigma_i|^4$, while the mixing between different species, $(h_i h_j/4)\sigma_i^2\sigma_j^{\dagger 2}$ gives rise to the higher-order 'sunset' diagram in Fig. 2, proportional to $h^4 {N_Y}^2$. To obtain the physical σ_i-mass one needs to solve the associated gap equation, and to lowest

---

[2] Note that the relevant two-point correlation function for a complex scalar is $\langle \sigma_i \sigma_i^\dagger \rangle$, which receives distinct contributions from the quartic and bi-quadratic interaction terms.

order we have [37, 38]:

$$\left(\frac{m_\sigma}{T}\right)^2 = \left(\frac{m_0}{T}\right)^2 + \frac{m_\sigma^2 h^2}{16\pi^2}\left[\log\left(\frac{m_\sigma^2}{\mu^2}\right) - 1\right] + \frac{h^2}{2\pi^2}\int_0^\infty dx \frac{x^2}{\sqrt{x^2 + (m_\sigma/T)^2}} \frac{1}{e^{\sqrt{x^2+(m_\sigma/T)^2}} - 1} , \tag{3.2}$$

where we have omitted the field index for simplicity, m_0 denotes its bare mass and μ is the renormalization scale, with the physical mass evaluated at $\mu = m_\sigma$. For small couplings, the hard thermal loop approximation yields $m_\sigma^2 \simeq m_0^2 + h^2T^2/12$. We have solved the gap equation numerically for different values of m_0/T, the results being illustrated in Fig. 3.

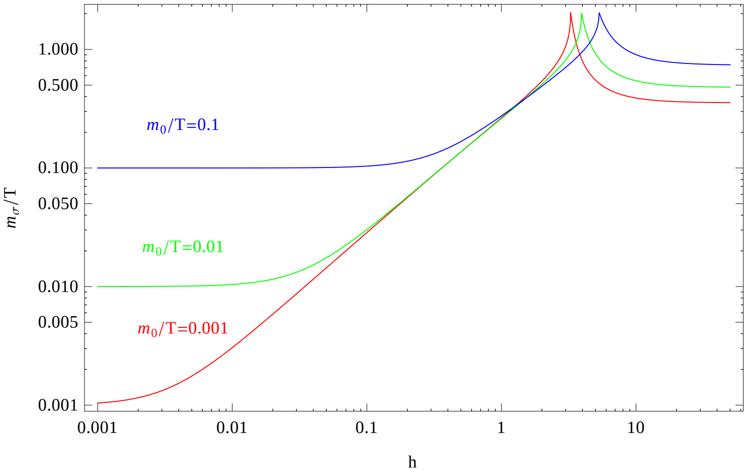

FIG. 3: Numerical solution of the gap equation for the mass of the σ_i scalars as a function of the coupling $h_i = h$ for different values of the tree-level mass parameter m_0/T.

As can be seen in Fig. 3, the hard thermal loop approximation holds for $h \lesssim \mathcal{O}(1)$, and for large couplings the mass tends to a constant value, which is well described by the expression:

$$\frac{m_\sigma}{T} \simeq \frac{\pi}{2 - \ln(m_0^2/T^2)} . \tag{3.3}$$

This shows that, for $m_0 \lesssim T$, we expect $m_\sigma \lesssim T$ for all values of the coupling constant. This was expected due to the Boltzmann-factor in the loop integral, which precludes a large mass being generated by large couplings. Of course the one-loop approximation is not an accurate estimate for large couplings, but this result should hold at all orders in perturbation theory, including the 'sunset' contributions that may involve a large field multiplicity, as all loop diagrams involve this Boltzmann-suppression. Moreover, higher-order loop contributions do not have a definite sign [37], which implies a slower growth of m_σ/T with the coupling constant and field multiplicities.

The tree-level masses of the fields in the Y_i-multiplets have, of course, a model-dependent value, and may be generated by a variety of both supersymmetric and non-supersymmetric effects which are not directly related to the inflationary dynamics. However, if for example this sector includes the MSSM fields, we expect these masses to vanish or to at least be extremely small compared to the high temperatures typical of warm inflation models, $T \gg \mathcal{O}(\text{TeV})$ [15]. Given the above considerations, this will also be the case when thermal corrections are included, so that we will take $m_\sigma \lesssim T$ in computing the associated dissipation coefficient.

IV. DISSIPATION COEFFICIENT

The coupling between the inflaton and the χ, ψ_χ fields induces time non-local corrections to the inflaton effective action which, in the adiabatic regime, where $\dot\varphi/\varphi \ll \Gamma_\chi$, with the latter denoting the χ decay width, lead to the effective friction term $\Upsilon\dot\varphi$ in the inflaton's equation motion [35]. As mentioned above, these dissipative effects are due to the finite decay width of the X-multiplet fields, and correspond to an effective production of relativistic degrees of freedom, yielding a non-zero imaginary part for the self-energy of the fields in the Y_i-sector [39].

The leading contribution to the dissipation coefficient from the complex scalar χ-modes arises at one-loop order, as illustrated in Fig. 4, and has the following form [35]:

$$\Upsilon = \frac{4}{T}\left(\frac{g^2}{2}\right)^2 \varphi^2 \int \frac{d^4p}{(2\pi)^4} \rho_\chi^2 n_B(1+n_B) \ , \tag{4.1}$$

where $n_B(p_0) = [e^{p_0/T} - 1]^{-1}$ is the Bose-Einstein distribution.

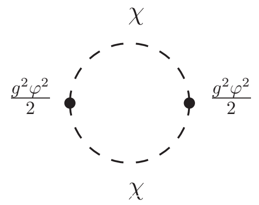

FIG. 4: Feynman diagram contributing to the inflaton effective action at leading order.

The spectral functions for the χ-fields correspond to the fully dressed propagators, including the effect of their finite decay width into σ_i-particles:

$$\rho_\chi(p_0, p) = \frac{4\omega_p \Gamma_\chi}{(p_0^2 - \omega_p^2)^2 + 4\omega_p^2 \Gamma_\chi^2} \ , \tag{4.2}$$

where $\omega_p = \sqrt{\tilde{m}_\chi^2 + p^2}$ for modes of 3-momentum $|\mathbf{p}| = p$ and energy p_0. The contribution from the ψ_χ-modes is given by an analogous expression with fermionic propagators and the relevant couplings, but has been shown to be suppressed in the low-temperature regime, $T \ll m_\chi$ [35], which is the main scope of this work. It should be noted that the dissipation coefficient receives positive contributions from both the bosonic and fermionic fields that are directly coupled to the inflaton, so that only the time-local radiative corrections can be (partially) canceled by the underlying supersymmetry of the model. The suppression of the fermionic contribution is also a symptom of supersymmetry breaking during warm inflation, due to both the finite inflaton energy density and the finite temperature of the radiation bath.

The decay width of the χ bosons also includes contributions from both the bosonic and fermionic final states in the Y_i-multiplets. The temperature and inflaton field dependence of the partial decay widths is also different for bosons and fermions [35], and again the fermionic contibutions are sub-leading. Taking also into account our earlier discussion of thermalization rates in the Y_i-sector, it is clear that only the complex scalar fields χ and σ_i are relevant to the dynamics of warm inflation, and that the underlying supersymmetry is only manifest in the logarithmic form of the radiative corrections to the inflaton potential in Eq. (2.5).

The leading process contributing to the decay width of the χ fields is then the two-body decay $\chi \to \sigma_i \sigma_i$ (and the complex conjugate process), and at finite temperature we include contributions from both decays and inverse decays, as well as thermal scatterings off particles in the radiation bath. This has been computed in [35] from the imaginary part of the χ-self energy at one-loop order, yielding:

$$\Gamma_\chi = \frac{h^2 N_Y}{64\pi} \frac{m_\chi^2}{\omega_p} F_T(p, p_0) \ , \tag{4.3}$$

where

$$\begin{aligned} F_T(p,p_0) \ &= \ \left[\frac{\omega_+ - \omega_-}{p} + \frac{T}{p}\log\left(\frac{1-e^{-\frac{\omega_+}{T}}}{1-e^{-\frac{\omega_-}{T}}}\frac{1-e^{-\frac{p_0-\omega_-}{T}}}{1-e^{-\frac{p_0-\omega_+}{T}}}\right)\right]\theta\left(p_0^2 - p^2 - 4m_\sigma^2\right) + \\ &+ \ \left[\frac{T}{p}\log\left(\frac{1-e^{-\frac{\omega_+}{T}}}{1-e^{-\frac{\omega_-}{T}}}\frac{1-e^{-\frac{p_0+\omega_-}{T}}}{1-e^{-\frac{p_0+\omega_+}{T}}}\right)\right]\theta\left(-p_0^2 + p^2\right) \ , \end{aligned} \tag{4.4}$$

with $\theta(x)$ denoting the Heaviside function and

$$\omega_\pm = \sqrt{k_\pm^2 + m_\sigma^2} \ , \qquad k_\pm = \frac{1}{2}\left|p \pm p_0\left(1 - \frac{4m_\sigma^2}{p_0^2 - p^2}\right)^{\frac{1}{2}}\right| \ . \tag{4.5}$$

Note that the factor m_χ^2 appearing in Eq. (4.3) arises from the fact that the coupling between the χ and σ_i fields depends on the inflaton vev, whereas for the physical mass of the heavy bosons we use the renormalized mass $\tilde{m}_\chi$. Also, the first term in Eq. (4.4) corresponds to direct and inverse decays, while the second Landau-damping term is associated to thermal scatterings.

From Eqs. (4.1-4.3), it is easy to see that the dissipation coefficient depends on the mass of χ fields, m_χ/T, and the effective coupling, $\hat{h} = h\sqrt{N_Y}$, up to an overall rescaling by the coupling g^2. We have integrated Eq. (4.1) numerically for different values of these parameters, and we show a representative selection of our results in Fig. 5.

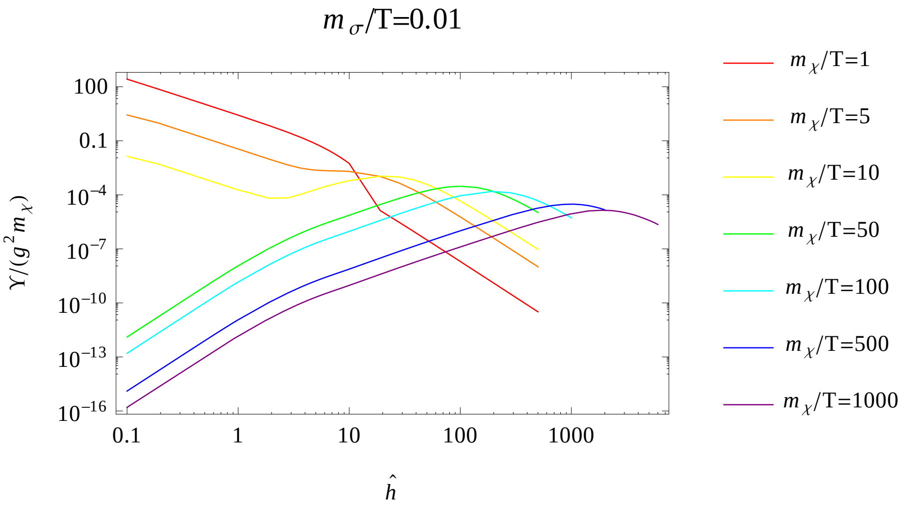

FIG. 5: Numerical results for the dissipation coefficient as a function of the effective coupling $\hat{h} = h\sqrt{N_Y}$ for different values of m_χ/T. These results correspond to $m_\sigma/T = 0.01$.

As one can easily conclude from the results shown in Fig. 5, the dependence on the effective coupling $\hat{h}$ is non-trivial, exhibiting a distinct behavior for small and large couplings depending on the mass of the χ fields. As we will discuss below, these correspond to two different contributions to the integral in Eq. (4.1) that can be analyzed separately and, in fact, represent different physical processes.

A. Low momentum contribution

For $m_\chi/T \gtrsim 10$ and the range of values of the effective coupling shown in Fig. 5, the main contribution to the dissipation coefficient comes from *virtual* χ modes with low momentum and energy, $p, p_0 \ll m_\chi$, so that one can use the approximation $(p_0^2 - \omega_p^2)^2 \simeq \tilde{m}_\chi^4$. If, in addition, these modes have a narrow width and thermal mass corrections can be neglected, $\Gamma_\chi \ll \tilde{m}_\chi \sim m_\chi$, the spectral function takes the simple form $\rho_\chi \simeq 4\Gamma_\chi/m_\chi^3$ and it is easy to see that:

$$\frac{\Upsilon^{LM}}{g^2 m_\chi} = A\hat{h}^4 \left(\frac{T}{m_\chi}\right)^3 . \tag{4.6}$$

The constant can be determined from the numerical data and one obtains $A \simeq 1.63 \times 10^{-3}$ for $m_\sigma/T = 0.01$, consistently with the results obtained in [34, 35], taking into account our choice of normalization in Eq. (2.1). This behavior corresponds to $\hat{h} \lesssim 1$ for $m_\chi/T \gtrsim 10$. It is convenient to write this in the form:

$$\Upsilon^{LM} = C_\phi \frac{T^3}{\varphi^2} , \qquad C_\phi = 0.00325\hat{h}^4 . \tag{4.7}$$

However, as one increases the effective coupling $\hat{h}$, the finite width of the χ fields and their thermally-induced mass become significant, and the dissipation coefficient grows slower than $\hat{h}^4$ for $\hat{h} \gtrsim 1$. Although the exact dependence cannot be determined analytically, the numerical data is well described by including a polynomial correction factor in Eq. (4.6), motivated by the Γ_χ-dependence of the loop integral in Eq. (4.1) and the form of the renormalized mass $\tilde{m}_\chi$:

$$\frac{\Upsilon^{LM}}{g^2 m_\chi} = \frac{A\hat{h}^4}{f(\hat{h}, m_\chi/T, m_\sigma/T)}\left(\frac{T}{m_\chi}\right)^3 , \qquad f(\hat{h}, m_\chi/T, m_\sigma/T) = 1 + \sum_{n=1}^{4} \alpha_{2n}\hat{h}^{2n} , \tag{4.8}$$

where $\alpha_n = \alpha_n(m_\chi/T, m_\sigma/T)$ and $A = A(m_\sigma/T)$. We have performed a numerical fit to the data using this expression in order to obtain the value and mass-dependence of these coefficients, by varying m_χ/T for fixed m_σ/T and vice-versa. The results for $m_\sigma/T = 0.01$ are illustrated in Fig. 6, while the results for $m_\chi/T = 50$ are shown in Fig. 7.

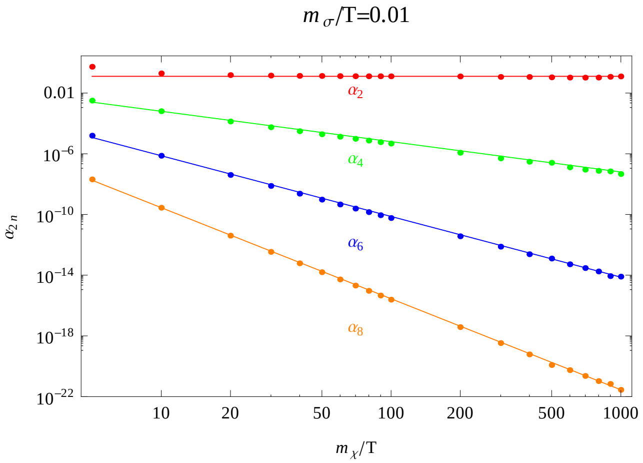

FIG. 6: Coefficients of the polynomial correction to the low-momentum dissipation coefficient for different values of m_χ/T and $m_\sigma/T = 0.01$. The solid lines represent the best fit curve in each case.

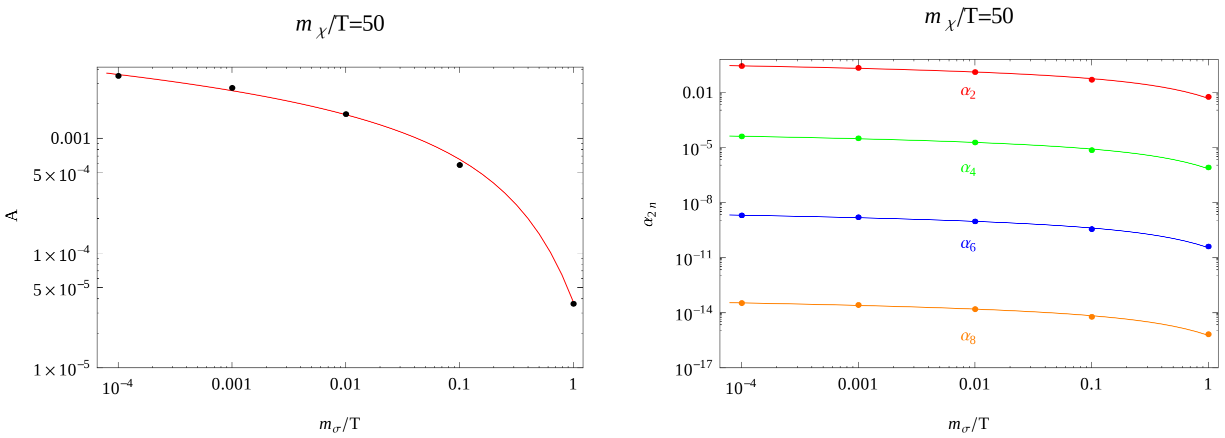

FIG. 7: Overall normalization and coefficients of the polynomial correction to the low-momentum dissipation coefficient for different values of m_σ/T and $m_\chi/T = 50$. The solid lines represent the best fit curve in each case.

From these results one can deduce the following approximate form for the polynomial coefficients and the overall normalization constant:

$$\frac{\Upsilon^{LM}}{g^2 m_\chi} \simeq \frac{4.3\times 10^{-4}\hat{h}^4 |\log(1-e^{-\frac{5}{2}\frac{m_\sigma}{T}})|}{1+\left[0.03\hat{h}^2 + 0.02\hat{h}^4\left(\frac{m_\chi}{T}\right)^{-2} + 0.002\hat{h}^6\left(\frac{m_\chi}{T}\right)^{-4} + 7\times 10^{-5}\hat{h}^8\left(\frac{m_\chi}{T}\right)^{-6}\right]|\log(1-e^{-2\frac{m_\sigma}{T}})|}\left(\frac{T}{m_\chi}\right)^3 . \tag{4.9}$$

The expression (4.9) is valid for $m_\chi/T \gtrsim 10$, while for lower values one observes larger deviations from the best fit result, in particular for the lowest coefficient α_2, which exhibits a mild dependence on m_χ/T. This is due to contributions from real χ-modes, which become significant for lighter χ-fields and smaller couplings and that we will analyze in the next section.

An important feature of these results is the mild logarithmic dependence on m_σ/T, and for practical purposes its is useful to evaluate this in the limit $m_\sigma \ll T$, for which we obtain:

$$\Upsilon^{LM} \simeq \frac{0.015\hat{h}^2}{1+0.53\hat{h}^2\left(\frac{m_\chi}{T}\right)^{-2}+0.07\hat{h}^4\left(\frac{m_\chi}{T}\right)^{-4}+0.002\hat{h}^6\left(\frac{m_\chi}{T}\right)^{-6}}\frac{T^3}{\varphi^2} \ . \tag{4.10}$$

In this limit and for $m_\chi/T \gtrsim \hat{h}$, we recover an expression for the dissipation coefficient of the form in Eq. (4.7):

$$\Upsilon^{LM} \simeq C_\phi \frac{T^3}{\varphi^2} \ , \qquad C_\phi \simeq 0.03h^2 N_Y \ . \tag{4.11}$$

Eq. (4.11) is one of our main results, showing that, for large values of the effective coupling in the narrow width regime, the dissipation constant grows like $C_\phi \propto h^2 N_Y$ and not as $h^4 N_Y^2$ as obtained in [34, 35] and which is valid only for $\hat{h} \lesssim 1$. In Fig. 8 we also plot the effective function $C_\phi(m_\chi/T, m_\sigma/T)$ valid for $m_\chi/T \gtrsim 10$, illustrating how it becomes constant for $m_\chi/T \gtrsim \hat{h}$ and also showing that the dependence on m_σ/T is negligible for large values of the effective coupling.

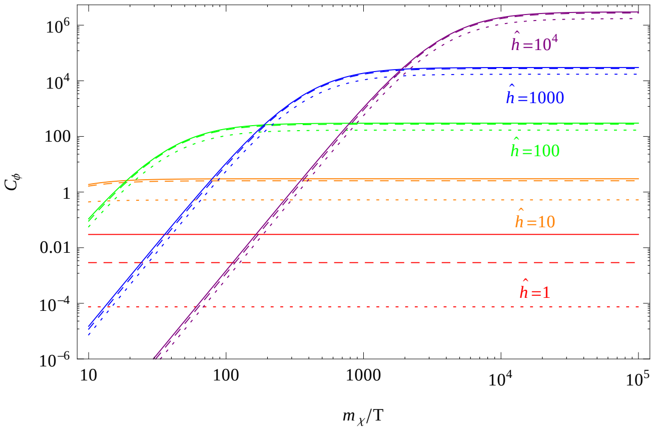

FIG. 8: The dissipation function $C_\phi(m_\chi/T, m_\sigma/T)$ as a function of m_χ/T for different values of the effective coupling $\hat{h} = h\sqrt{N_Y}$ and for $m_\sigma/T \to 0$ (solid), $m_\sigma/T = 0.01$ (dashed) and $m_\sigma/T = 1$ (dotted), using the best fit expression in Eq. (4.9).

On the other hand, when $m_\chi/T \lesssim \hat{h}$, the effects of the width of the χ fields become important and suppress the dissipation coefficient, as illustrated in Fig. 8 by the sharp decrease in C_ϕ. In the broad width limit, where the term with coefficient α_8 is the leading polynomial correction, we have for $m_\sigma \ll T$:

$$\Upsilon^{LM} \simeq 0.94\frac{g^6}{h^4 N_Y^2}\frac{\varphi^4}{T^3} \ . \tag{4.12}$$

B. Pole contribution

The contribution to the dissipation coefficient from *real* χ-modes is generically Boltzmann-suppressed, so that previous analysis assumed that it only becomes relevant in the high-temperature limit, $T \gg m_\chi$. However, our numerical results suggest that the Boltzmann suppression factor $e^{-m_\chi/T}$ may be compensated by a sufficiently small effective coupling in the low-temperature regime, so that on-shell modes become the dominant contribution to the dissipation coefficient, as can be seen in Fig. 5 for $m_\chi/T \lesssim 10$. To better understand this, let us expand the spectral function in Eq. (4.2) about its pole at $p_0 \simeq \omega_p$, which corresponds to the production of on-shell modes. We then obtain:

$$\Upsilon^P = \frac{2}{T}\left(\frac{g^2}{2}\right)^2 \varphi^2 \int \frac{d^3p}{(2\pi)^3}\frac{1}{\Gamma_\chi \omega_p^2} n_B(1+n_B) \ , \tag{4.13}$$

from which it is clear that $\Upsilon \propto \hat{h}^{-2}$, a behavior that is evident in Fig. 5 in the small effective coupling region. Proceeding as in the previous section, we have performed a numerical fit to the data in this region to an expression of the form:

$$\frac{\Upsilon^P}{g^2 m_\chi} = B(m_\chi/T, m_\sigma/T)\hat{h}^{-2} \ . \tag{4.14}$$

The dependence on the mass of the light fields is actually negligible in this case for $m_\sigma \lesssim T$, and in Fig. 9 we illustrate our results for $m_\sigma/T = 0.01$.

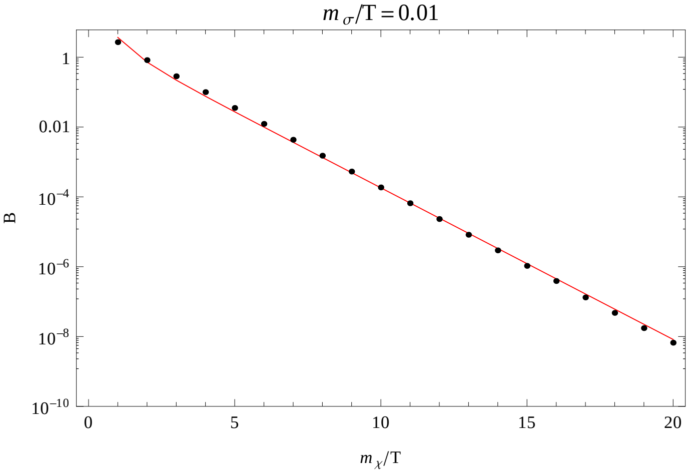

FIG. 9: Value of $B(m_\chi/T)$ in the pole approximation for $m_\sigma/T = 0.01$. The solid red line corresponds to the fitting function $B(x) = 4e^x/(e^x - 1)^2$.

The coefficient B exhibits a strong dependence on m_χ/T, which is mainly due to the Bose-Einstein factors in Eq. (4.1), so that the dissipation coefficient can in this case be well approximated by:

$$\Upsilon^P \simeq \frac{4g^2}{\hat{h}^2}\frac{m_\chi e^{m_\chi/T}}{(e^{m_\chi/T} - 1)^2} \ . \tag{4.15}$$

One should note that even though on-shell modes can give the dominant contribution to the dissipation coefficient for sufficiently small effective coupling, the width of the χ-fields may be very small in this limit, which implies that the adiabatic condition $\dot{\varphi}/\varphi \ll \Gamma_\chi$ may no longer hold, which needs to be taken into account when constructing models of warm inflation in this limit. Also, it has been shown that a full resummation of ladder diagrams contributing at the same order to the dissipation coefficient is required in this limit, although this does not generically change its order of magnitude [40].

C. Full dissipation coefficient

While previously we have analyzed the contributions from virtual and real modes of the χ field separately, the full dissipation coefficient is well described by adding both contributions, in Eqs. (4.9) and (4.15), as illustrated in Fig. 10 for $m_\chi/T = 10$.

In the limit $m_\sigma \ll T$, we may then write the following expression for the dissipation coefficient:

$$\frac{\Upsilon}{g^2 T} \simeq \frac{4}{\hat{h}^2}\left(\frac{m_\chi}{T}\right)\frac{e^{m_\chi/T}}{(e^{m_\chi/T} - 1)^2} + \frac{0.015\hat{h}^2}{1 + 0.53\hat{h}^2\left(\frac{m_\chi}{T}\right)^{-2} + 0.07\hat{h}^4\left(\frac{m_\chi}{T}\right)^{-4} + 0.002\hat{h}^6\left(\frac{m_\chi}{T}\right)^{-6}}\left(\frac{T}{m_\chi}\right)^2 \ . \tag{4.16}$$

In Fig. 11 we plot this expression by varying m_χ/T and keeping $\hat{h}$ fixed, which is more useful for practical implementations of warm inflation given that the former depends on the ratio φ/T, which is (slowly) varying during inflation.

The curves shown in Fig. 11 clearly illustrate the different regimes analyzed earlier, with the low-momentum (pole) contribution dominating at large (small) masses. It is also clear that for large values of $\hat{h}$ the contribution from virtual

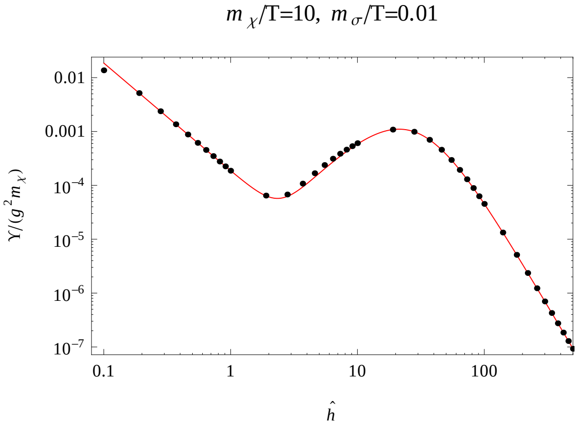

FIG. 10: Comparison between the numerical results and the best fit expression obtained by adding the low-momentum and pole contributions to the loop integral for $m_\chi/T = 10$ and $m_\sigma/T = 0.01$.

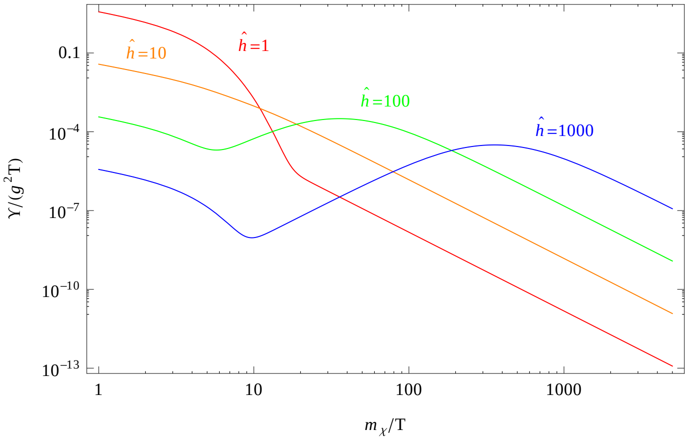

FIG. 11: Full dissipation coefficient as a function of m_χ/T for different values of the effective coupling $\hat{h} = h\sqrt{N_Y}$, using the expression inferred from the numerical results.

modes is different depending on whether their decay width is small or large compared to the mass, with the narrow width regime corresponding to the monotonic $(T/m_\chi)^2$-behavior at large masses.

Given that during slow-roll inflation m_χ/T may not vary significantly, it is possible for the narrow-width form of the low-momentum dissipation coefficient in Eq. (4.11) to hold during the full inflationary trajectory. In general, however, one expects transitions between the different regimes to take place over the $40 - 60$ e-folds of inflationary expansion, and the dissipation coefficient may not have a monotonic behavior as illustrated in Fig. 11. Nevertheless, it should be emphasized that the contributions from real and virtual modes may actually have comparable values, although for different values of m_χ/T.

V. HIGHER-ORDER CORRECTIONS

In implementations of warm inflation based on the superpotential in Eq. (2.1), one typically finds that large values of the constant $C_\phi \gtrsim 10^5 - 10^6$ are required for a sufficiently long period of inflation (see e.g. [15]). Although some of the assumptions used in these models may be relaxed, such as for example assuming that all MSSM degrees of freedom are present in the thermal bath during inflation, our previous discussion shows that large values of the effective coupling $\hat{h} = h\sqrt{N_Y}$ are generically required, unless an unnaturally large number of X-multiplets is coupled to the inflaton field. Note that, in this latter case, radiative corrections to the inflaton potential may still be kept under control by tuning the coupling g, which does not modify the dissipation coefficient in the low-momentum and narrow width regime [see e.g. Eqs. (4.7) and (4.11)].

It is then natural to investigate how higher-order corrections modify our earlier discussion and, in particular, the computation of the dissipation coefficient. Firstly, as we have discussed earlier, the condition $m_\sigma \lesssim T$ should hold for large couplings and field multiplicities, and in fact the next-to-leading-order corrections come from the 'sunset' diagram shown in Fig. 2 and are proportional to $h^4 N_Y = h^2\hat{h}^2$, which can be made small in the limit of small couplings and large multiplicities such that $\hat{h}$ remains large. Similarly, the next-to-leading order corrections to the mass of the heavy fields, $\tilde{m}_\chi$, arising from the bi-quadratic and quartic interactions of the σ_i fields, are $\mathcal{O}(h^4 N_Y, h^6 N_Y^2)$ and can also be made small in this limit. Moreover, for large tree-level masses, $m_\chi \gtrsim T$, thermal corrections are negligible up to large values of the effective coupling.

The most relevant effect of higher-order corrections are, in fact, modifications to the decay width of the χ-fields due to the self-interactions in the light scalar sector. These allow for emission of additional scalar pairs in the final decay state, with $\chi \to \sigma_i\sigma_i^\dagger(\sigma_j\sigma_j)(\sigma_k\sigma_k)\ldots, i, j, k, \ldots = 1, \cdots N_Y$, which will necessarily increase the total decay width. The effect of these higher-order many-body final states is hard to estimate in general due to the complexity of the resulting phase space, but to estimate this we have computed the leading corrections from four-body decays for on-shell bosons at zero temperature. We describe this computation in detail in Appendix A, yielding a 'radiator' factor relative to the two-body partial decay width $\Gamma_\chi = R\Gamma_\chi^{(2)}$ of the form:

$$R = 1 + \frac{2}{9}\left(\frac{h}{4\pi}\right)^4 N_Y + \ldots\ , \tag{5.1}$$

for $N_Y \gg 1$. The leading correction is thus also proportional to $h^4 N_Y$, so that it may be neglected for $h \ll 1$ even though $\hat{h} \gtrsim 1$.

On the other hand, for $(h/4\pi)^4 N_Y \gtrsim 1$, we expect the radiator factor to become large, with significant contributions from an increasing number of many-body final states. Finite temperature effects may also increase this factor, as suggested by the leading order result in Eq. (4.4). By enhancing the decay width, these corrections will also increase the dissipation coefficient in the narrow-width regime, as suggested by the results derived in the previous section. Although a full determination of the radiator factor is outside the scope of this work, we expect our results in this regime to be modified by replacing $\hat{h}^2 \to \hat{h}^2 R$, with the narrow width expressions now holding for $m_\chi/T \gtrsim \hat{h}\sqrt{R}$, in which case the higher-order corrections to $\tilde{m}_\chi$ have a negligible effect according to the above discussion. In fact, one should note that $(h/4\pi)^4 N_Y$ must not be too small or otherwise the thermalization rate of the light scalars will be suppressed, according to Eq. (2.7), which suggests further exploitation of higher-order radiative corrections in the light scalar sector.

VI. CONCLUSION

In this work we have extended earlier analyses of dissipative effects in supersymmetric warm inflation in the low-temperature regime, $m_\chi \lesssim T$, to generic couplings and field multiplicities. As found in earlier analyses, the dissipation coefficient arising from the two-stage scalar interactions $\phi \to \chi \to \sigma_i$ differs significantly depending on whether the heavy fields χ are produced on- or off-shell. We have computed the dissipation coefficient numerically and obtained expressions that accurately describe our numerical results in both cases. Our full result, corresponding to a sum of both real and virtual contributions, is given by Eq. (4.16) in the limit $m_\sigma \ll T$. We also find that the dissipation coefficient exhibits only a mild logarithmic dependence on the mass of the light fields, with $m_\sigma \lesssim T$ even for large values of the coupling constant.

We have found that, for a given value of the effective coupling $\hat{h} = h\sqrt{N_Y}$, the production of on-shell χ-modes from the rolling inflaton field is the dominant source of dissipation in the small mass limit, $m_\chi/T \lesssim 10$, consistently with earlier analysis. For larger masses, the dominant process is the production of virtual χ-pairs which then decay into the light degrees of freedom. In this case, the dissipation coefficient takes different forms depending on whether the field has a narrow or broad decay width, yielding $\Upsilon \simeq C_\phi T^3/\varphi^2$ and $\Upsilon \simeq D_\phi \varphi^4/T^3$, respectively. Although in the narrow width regime we obtain $C_\phi \propto \hat{h}^4$ for $\hat{h} \lesssim 1$ and finite m_σ/T, in agreement with [34, 35], we find $C_\phi \propto \hat{h}^2$ for large effective couplings, which is the regime where dissipative effects may be more pronounced. This constant is also enhanced by the multiplicity of the heavy fields, N_X, and by radiative corrections leading to many-body decay channels, yielding a radiator factor R that we have estimated to leading order. Taking all these considerations into account, we have:

$$C_\phi \simeq 4.7\left(\frac{h}{4\pi}\right)^2 R N_X N_Y\ , \tag{6.1}$$

with the narrow width approximation holding for $m_\chi/T \gtrsim h\sqrt{N_Y R}$. Notice that in this regime the dissipation coefficient is independent of the coupling g between the inflaton and the heavy fields, which allows for large dissipative effects, while keeping radiative and thermal corrections to the inflaton potential under control. Moreover, this shows that strong dissipative effects may be achieved by moderately large field multiplicities and couplings. In particular we expect radiative corrections to become significant for $(h/4\pi)^4 N_Y \gtrsim 1$, which may in fact allow for warm inflation models with a small number of fields.

Finally, one should emphasize that, despite the supersymmetric nature of the underlying model, interactions in the fermionic sector are inherently different from the scalar particles, as a consequence of supersymmetry breaking at finite temperature and energy density during warm inflation. In particular, both the dissipative production and the thermalization rate for light fermionic degrees of freedom are suppressed for $m_\chi/T \gtrsim 1$, so that fermions are a negligible (and most probably non-thermal) component of the radiation bath during inflation. We nevertheless expect fermions to be produced once the mass of χ and ψ_χ has decreased sufficiently towards the end of inflation, which may happen in models where φ decreases or when there are additional tachyonic contributions to m_χ, as in hybrid inflation models.

In this work, we have not considered the possible embedding of the supersymmetric model in Eq. (2.1) in a gauge theory, mainly for simplicity, since the inclusion of gauge fields make the analysis much more involved. However, for minimally coupled χ fields, we do not expect direct decays into gauge fields to be significant, since the only two-body process $\chi \to \chi\gamma$, although possible at finite temperature, is suppressed by the large χ mass. Note that gauge bosons may nevertheless be emitted from the σ scalars, if they are charged, or produced thermally, but this will necessarily involve a separate gauge coupling that can be made small enough for us to neglect these processes.

We have shown in this work that by further exploiting regimes of parameters involving not too large coupling constants, such that perturbation theory remains valid, or at least that higher-order corrections are not large enough to spoil the lowest-order predictions, it is possible to enlarge the parameter space useful for warm inflation model building, by allowing for stronger dissipation at the cost of not too large field degeneracies, while thermal corrections to the inflaton potential are still kept under control. Thus, we hope that this work will motivate further investigation of warm inflation model building and of the importance of dissipative effects in modern cosmological problems, both during and after the early inflationary phase.

Acknowledgments

J. G. R. would like to thank Einan Gardi and Jennifer Smillie for useful discussions. M. B. G. is partially supported by MICINN (FIS2010-17395) and "Junta de Andalucía" (FQM101). A. B. and J. G. R. are supported by STFC. R. O. R. is partially supported by research grants from Conselho Nacional de Desenvolvimento Científico e Tecnológico (CNPq) and Fundação Carlos Chagas Filho de Amparo à Pesquisa do Estado do Rio de Janeiro (FAPERJ).

Appendix A: Four-body decay at zero temperature

The leading correction to the decay width of the heavy χ fields arises from the 4-body decays $\chi \to \sigma_i \sigma_i^\dagger \sigma_j \sigma_j$, illustrated by the diagram below.

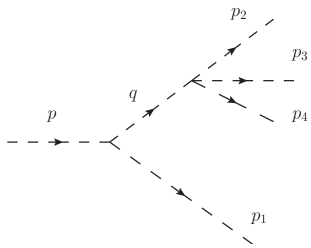

FIG. 12: Feynman diagram for the 4-body decay $\chi \to \sigma_i \sigma_i^\dagger \sigma_j \sigma_j$.

Here we will compute the associated partial decay width for an 'on-shell' heavy particle at $T = 0$. Assuming $h_i = h$ for simplicity, the corresponding amplitude is given by:

$$\mathcal{M}^{(4)} = -(m_\chi h^2) h^2 \frac{1}{q^2 - m_\sigma^2} \ , \tag{A1}$$

where $q^2 = (p - p_1)^2$ is the momentum transfer. For the kinematics of the decay we follow [41], so that:

$$d\Gamma^{(4)}_{\chi(ij)} = \frac{X\beta_{12}\beta_{34}}{4(4\pi)^6 m_\chi^3}\frac{2|\mathcal{M}_{(4)}|^2}{S_{ij}} ds_{12} ds_{34} d\cos\theta_1 d\cos\theta_3 d\phi \ , \tag{A2}$$

where $\beta_{12(34)}$ is the velocity of particle 1 (3) in the CM frame of particles 1 and 2 (3 and 4), $s_{12} = (p_1 + p_2)^2$, $s_{34} = (p_3 + p_4)^2$, $\theta_{1(3)}$ is the angle between $\mathbf{p}_{1(3)}$ and $\mathbf{p}_{1(3)} + \mathbf{p}_{2(4)}$ and ϕ is the angle formed by the planes $(\mathbf{p}_1, \mathbf{p}_2)$ and $(\mathbf{p}_3, \mathbf{p}_4)$. We have also defined:

$$X = \frac{1}{2}\sqrt{m_\chi^4 + s_{12}^2 + s_{34}^2 - 2m_\chi^2(s_{12} + s_{34}) - 2s_{12}s_{34}} \ . \tag{A3}$$

The symmetry factor S_{ij} accounts for the number of identical bosons in the final state, with $S = 3!$ for $i = j$ and $S = 2!$ for $i \neq j$, and we multiply the squared amplitude by a factor 2 to account for the fact that the $\sigma_j\sigma_j$ pair may emitted from either primary σ_i field.

For simplicity, we take the limit $m_\sigma \to 0$, in which we can show the following kinematical relations:

$$\begin{aligned} E_1 + E_2 &= \frac{m_\chi^2 + s_{12} - s_{34}}{2m_\chi} \ , \\ s_{12} &= 2E_1(E_1 + E_2 - |\mathbf{p}_{12}|\cos\theta_1) \ , \\ |\mathbf{p}_{12}| &= |\mathbf{p}_1 + \mathbf{p}_2| = \sqrt{(E_1 + E_2)^2 - s_{12}} \ . \end{aligned} \tag{A4}$$

These then allow one to write:

$$q^2 = m_\chi^2 - 2m_\chi E_1 = m_\chi^2\left(\frac{m_\chi^2 - s_{12} - s_{34} - 2m_\chi\cos\theta_1|\mathbf{p}_{12}|}{m_\chi^2 + s_{12} - s_{34} - 2m_\chi\cos\theta_1|\mathbf{p}_{12}|}\right) \ . \tag{A5}$$

Hence, $q^2 = q^2(s_{12}, s_{34}, \cos\theta_1)$, so that the integrals in θ_3 and ϕ are trivial. The remaining integrals can be performed by taking into account that $0 < s_{12} < m_\chi^2$, $0 < s_{34} < (m_\chi - \sqrt{s_{12}})^2$ and $-1 \leq \cos\theta_1 \leq 1$.

The integrals actually exhibit logarithmic divergences in the limit $m_\sigma \to 0$, corresponding to the case where the secondary emitted scalars are soft and collinear with one of the primary scalars. As for example in QED and QCD, these soft collinear divergences will cancel against contributions from virtual scalars, i.e. when the $\sigma_j\sigma_j$ pair is emitted and re-absorbed (see e.g. [42]), a result which should hold also at finite temperature [43]. Keeping only the finite terms and summing over all possible decay channels, we obtain:

$$\Gamma_\chi^{(4)} = \frac{2}{27}(3N_Y - 2)\left(\frac{h}{4\pi}\right)^4\Gamma_\chi^{(2)} \ , \tag{A6}$$

where $\Gamma_\chi^{(2)}$ is given by the zero-temperature limit of Eq. (4.3) for an on-shell χ boson.

[1] A. H. Guth, Phys. Rev. D **23**, 347 (1981); A. Albrecht, P. J. Steinhardt, Phys. Rev. Lett. **48**, 1220 (1982); A. D. Linde, Phys. Lett. B **108**, 389 (1982).

[2] A. D. Linde, Phys. Rev. D **49**, 748 (1994) [astro-ph/9307002].

[3] E. J. Copeland, A. R. Liddle, D. H. Lyth, E. D. Stewart and D. Wands, Phys. Rev. D **49**, 6410 (1994) [astro-ph/9401011].

[4] A. Berera, L. -Z. Fang, Phys. Rev. Lett. **74**, 1912-1915 (1995) [astro-ph/9501024]; A. Berera, Phys. Rev. Lett. **75**, 3218 (1995) [astro-ph/9509049].

[5] A. Berera, Phys. Rev. D **54**, 2519 (1996) [hep-th/9601134].

[6] L. Z. Fang, Phys. Lett. B **95**, 154-156 (1980); I. G. Moss, Phys. Lett. B **154**, 120 (1985); J. Yokoyama, K. -i. Maeda, Phys. Lett. B **207**, 31 (1988).

[7] A. Berera, Nucl. Phys. B **585**, 666 (2000) [hep-ph/9904409].

[8] A. N. Taylor and A. Berera, Phys. Rev. D **62**, 083517 (2000) [astro-ph/0006077].

[9] L. M. Hall, I. G. Moss and A. Berera, Phys. Rev. D **69**, 083525 (2004) [astro-ph/0305015].

[10] I. G. Moss and C. Xiong, JCAP **0811**, 023 (2008) [arXiv:0808.0261 [astro-ph]].

[11] S. Gupta, A. Berera, A. F. Heavens and S. Matarrese, Phys. Rev. D **66**, 043510 (2002) [astro-ph/0205152].

[12] B. Chen, Y. Wang and W. Xue, JCAP **0805**, 014 (2008) [arXiv:0712.2345 [hep-th]].

[13] I. G. Moss and C. Xiong, JCAP **0704**, 007 (2007) [astro-ph/0701302].

[14] I. G. Moss and T. Yeomans, JCAP **1108**, 009 (2011) [arXiv:1102.2833 [astro-ph.CO]].

[15] M. Bastero-Gil and A. Berera, Int. J. Mod. Phys. A **24**, 2207 (2009) [arXiv:0902.0521 [hep-ph]].

[16] A. Berera, T. W. Kephart, Phys. Rev. Lett. **83**, 1084-1087 (1999) [hep-ph/9904410]; M. Bastero-Gil *et al.*, arXiv:0904.2195 [astro-ph.CO]; Y. -F. Cai, J. B. Dent and D. A. Easson, Phys. Rev. D **83**, 101301 (2011) [arXiv:1011.4074 [hep-th]].

[17] M. Bastero-Gil, A. Berera and J. G. Rosa, Phys. Rev. D **84**, 103503 (2011) [arXiv:1103.5623 [hep-th]].

[18] A. Hosoya and M. Sakagami, Phys. Rev. D **29**, 2228 (1984).

[19] M. Morikawa and M. Sasaki, Phys. Lett. B **165**, 59 (1985).

[20] M. Morikawa, Phys. Rev. D **33**, 3607 (1986).

[21] B. L. Hu, J. P. Paz and Y. Zhang, in *The Origin of Structure in the Universe*, Ed. E. Gunzig and P. Nardone (Kluwer Acad. Publ. 1993); E. Calzetta and B. L. Hu, Phys. Rev. D **49**, 6636 (1994); *ibid* **52**, 6770 (1995); B. L. Hu and A. Matacz, Phys. Rev. D **51**, 1577 (1995); A. Matacz, Phys. Rev. D **55**, 1860 (1997); S. A. Ramsey and B. L. Hu, Phys. Rev. D **56**, 678 (1997), Erratum-ibid. **57**, 3798 (1998).

[22] D. Lee and D. Boyanovsky, Nucl. Phys. B **406**, 631 (1993).

[23] D. Boyanovsky, H. J. de Vega, R. Holman, D. -S. Lee and A. Singh, Phys. Rev. D **51**, 4419 (1995).

[24] M. Gleiser and R. O. Ramos, Phys. Rev. D **50**, 2441 (1994).

[25] A. Berera, M. Gleiser, R. O. Ramos, Phys. Rev. D **58**, 123508 (1998) [arXiv:hep-ph/9803394 [hep-ph]].

[26] A. Ringwald, Ann. Phys. **177**, 129 (1987); Phys. Rev. D **36**, 2598 (1987).

[27] D. Boyanovsky, R. Holman and S. P. Kumar, Phys. Rev. D **56**, 1958 (1997).

[28] I. D. Lawrie, Phys. Rev. D **60**, 063510 (1999).

[29] A. Berera and R. O. Ramos, Phys. Rev. D **71**, 023513 (2005).

[30] J. Yokoyama, A. D. Linde, Phys. Rev. D **60**, 083509 (1999) [hep-ph/9809409].

[31] R. Herrera and M. Olivares, Int. J. Mod. Phys. D **21** (2012) 1250047 [arXiv:1205.2365 [gr-qc]]; R. Herrera and E. San Martin, Eur. Phys. J. C **71** (2011) 1701 [arXiv:1108.1371 [gr-qc]]; L. Visinelli, JCAP **1109** (2011) 013 [arXiv:1107.3523 [astro-ph.CO]]; H. Mishra, S. Mohanty and A. Nautiyal, Phys. Lett. B **710** (2012) 245 [arXiv:1106.3039 [hep-ph]]; P. Das and A. Deshamukhya, Indian J. Phys. **84** (2010) 617; R. Herrera, Phys. Rev. D **81** (2010) 123511 [arXiv:1006.1299 [astro-ph.CO]]. Y. Zhang, JCAP **0903** (2009) 023 [arXiv:0903.0685 [hep-ph]]; A. Deshamukhya and S. Panda, Int. J. Mod. Phys. D **18** (2009) 2093 [arXiv:0901.0471 [hep-th]].

[32] A. Berera, R. O. Ramos, Phys. Lett. B **567**, 294 (2003) [hep-ph/0210301].

[33] L. M. Hall and I. G. Moss, Phys. Rev. D **71**, 023514 (2005) [hep-ph/0408323].

[34] I. G. Moss and C. Xiong, hep-ph/0603266.

[35] M. Bastero-Gil, A. Berera and R. O. Ramos, JCAP **1109** (2011) 033 [arXiv:1008.1929 [hep-ph]].

[36] M. Bastero-Gil, A. Berera, R. O. Ramos and J. G. Rosa, Phys. Lett. B **712**, 425 (2012) [arXiv:1110.3971 [hep-ph]].

[37] L. Dolan and R. Jackiw, Phys. Rev. D **9**, 3320 (1974).

[38] M. B. Pinto and R. O. Ramos, J. Phys. A **39**, 6649 (2006) [cond-mat/0605508].

[39] I. G. Moss, C. M. Graham, Phys. Rev. D **78**, 123526 (2008) [arXiv:0810.2039 [hep-ph]].

[40] S. Jeon, Phys. Rev. D **47**, 4586 (1993) [hep-ph/9210227]; Phys. Rev. D **52**, 3591 (1995) [hep-ph/9409250].

[41] N. Quintero, G. Lopez Castro and D. Delepine, Phys. Rev. D **84**, 096011 (2011) [arXiv:1108.6009 [hep-ph]].

[42] M. E. Peskin and D. V. Schroeder, *An Introduction to Quantum Field Theory* (Westview Press, 1995).

[43] W. Keil, Phys. Rev. D **40**, 1176 (1989).